Available online at www.sciencedirect.com
ScienceDirect
Superlattices and Microstructures xx (xxxx) xxx–xxx
Superlattices and Microstructures
www.elsevier.com/locate/superlattices

Self-assembled ferromagnetic and superparamagnetic structures of hybrid Fe block copolymers

E. Sarantopoulou[a,*], J. Kovač[b], S. Pispas[a], S. Kobe[c], Z. Kollia[a], A.C. Cefalas[a]

[a] *National Hellenic Research Foundation, Theoretical and Physical Chemistry Institute, 48 Vassileos Constantinou Avenue, Athens 11635, Greece*
[b] *Jožef Stefan Institute, Department of Surface Engineering and Optoelectronics, Jamova 39, 1000 Ljubljana, Slovenia*
[c] *Jožef Stefan Institute, Department of Nanostructured Materials, Jamova 39, SI-1000 Ljubljana, Slovenia*

Abstract

Self-assembled 2D structures on thin films of block copolymers/Fe hybrid materials were fabricated on Si/Ta substrates, either by wet chemistry or laser irradiation at 157 nm. The polymer exhibits micelle-like structures with average dimensions of 5–10 nm and 30–50 nm for light and chemically reduced films respectively. For the laser processed films, SQUID measurements reveal a ferromagnetic response at 5 K, and 100 Oe coercivity was obtained for 2:1 iron concentration. For chemically reduced films, on the other hand, a superparamagnetic response with near zero coercivity at 5 K was obtained.

Keywords: Magnetic polymers; Ferromagnetic materials; Superparamagnetic materials; Self-assembly; Iron nanoparticles

1. Introduction

Nano-sized semiconductor and metal particles are utilized in tailoring electronic, optical, surface and magnetic applications [1–4]. Iron and iron oxide mesoscopic structures exhibit size-dependent magnetic, electronic, and catalytic properties. In particular, iron-containing nanoparticles have been used in magnetic and opto-magnetic applications [5,6], where the

* Corresponding author. Tel.: +30 21072738409; fax: +30 2107273842.
E-mail address: esarant@eie.gr (E. Sarantopoulou).

0749-6036/$ - see front matter © 2008 Published by Elsevier Ltd
doi:10.1016/j.spmi.2007.12.016

Please cite this article in press as: E. Sarantopoulou, et al., Self-assembled ferromagnetic and superparamagnetic structures of hybrid Fe block copolymers, Superlattices and Microstructures (2008), doi:10.1016/j.spmi.2007.12.016

magnetic spin flips due to a magnetic or electric field, and in drug delivery applications [7,8]. The importance of magnetic iron nanoparticles is based on the fact that they can be coated with biocompatible polymers during or after synthesis to prevent their biodegradation *in vivo* [9]. As iron particles are highly reactive, exhibiting spontaneous oxidation in air, their surfaces must be encapsulated either by a thin oxide layer or by a polymeric material. Metal ions in polymeric matrices tend to aggregate to form ionic cluster structures. These can further agglomerate to form metallic microphases that are well separated by the hydrophobic polymeric medium. These metallic ionic microdomains can be reduced chemically or through laser catalysis so that the size of the metallic agglomerations is reduced down to nanosize dimensions. The polymeric matrix prevents these metallic nanostructures from oxidation and large size agglomerations.

The common methods used to form metallic nanoparticles in polymeric matrices or surfactants are chemical reduction [10–13], photochemical reduction by γ irradiation [14] or UV/VUV irradiation [15,12], laser ablation [16], ion exchange [17], thermal annealing [18] and static casting [19].

The physical properties of metallic nanostructures depend on the size, shape and distribution of the particles. The size distribution and concentration are strongly correlated to the rate of reduction during the synthesis, the type and concentration of surfactants, the interactions at interfaces, the film thickness, and the presence of catalytic dopants [20–23].

Considerable effort has also been devoted to the preparation of 3D and 2D nanoparticle structures. Generally, the ability to assemble nanoparticles in multi-dimensional configurations requires controlled size distribution and balancing Van der Waals and dispersion forces [24, 25]. Furthermore, the synthesis of long selforganized iron chains driven by magnetic dipole interactions has been reported [26].

The appearance of self-assembled patterning greatly modulates the film properties and its response to external optical or magnetic fields. Diblock copolymers with hydrophilic and hydrophobic blocks, for example, exhibit phase separation into domains in solutions or in films [24,27]. Film morphology is greatly affected at the interfaces and depends on the film thickness.

As for the magnetic properties of iron nanoparticles in polymeric matrices, it has been reported that nano-sized particles formed by materials of macroscopic ferromagnetic response exhibit superparamagnetic behavior when they are assembled in the form of thin films [17,21, 22,28]. On the other hand, other investigations indicate that polymer-stabilized nanoparticles are ferromagnetic at room temperature rather than superparamagnetic [10,11].

In this work, thin films of block copolymer/iron hybrid materials [poly(styrene-b-2-vinylpyridine) (S2VP)/$FeCl_3$] containing self-assembled iron metal nanoparticle structures were synthesized by ionic polymerization [12]. We find a ferromagnetic response at 5 K arising from the Fe nanoparticle structures when the block copolymer has been reduced by vacuum ultraviolet (VUV) light at 157 nm. When the block copolymer has been chemically reduced, however, we observe a superparamagnetic response arising from the Fe nanoparticles in thin films of the same hybrid material. The enhancement of magnetic properties in the case of light reduction is due to restructuring of the micellar iron-like structures to smaller size iron nanostructures of 5–10 nm following 157 nm laser surface irradiation.

2. Experimental

A diblock copolymer of S2VP was synthesized by anionic polymerization under high vacuum using the sequential monomer addition technique. Styrene was polymerized first in

Please cite this article in press as: E. Sarantopoulou, et al., Self-assembled ferromagnetic and superparamagnetic structures of hybrid Fe block copolymers, Superlattices and Microstructures (2008), doi:10.1016/j.spmi.2007.12.016

tetrahydrofuran (THF), using n-BuLi as the initiator, followed by the addition of 2-vinylpyridine. Living anions were terminated by adding degassed methanol. The polymer was isolated after precipitation in hexane. Molecular weight (MW) and molecular weight distribution of the block copolymer were determined by size exclusion chromatography (SEC) using a Waters system, composed of a Waters 1515 isocratic pump, a set of three μ-Styragel mixed bed columns with a porosity range of 10^2–10^6 Å and a Waters 2414 refractive index detector (at 40 °C) controlled through Breeze software. Tetrahydrofuran was the mobile phase used at a flow rate of 1.0 ml/min at 30 °C. The set-up was calibrated with polystyrene (PS) standards having weight average molecular weights in the range 2500–900, 000 g/mol. Composition of the precursor diblocks was determined by ^{1}H-NMR spectroscopy using a Bruker AC300 instrument in $CDCl_3$ at 30 °C. The block copolymer used has MW $= 70,400$ g/mol, $MW/M_n = 1.01$ and PS composition 44 wt% [29].

Micelle formation takes place in a solution of toluene, a solvent that dissolves the PS blocks but not the 2VP blocks, leading to the formation of micelles with 2VP blocks in the core. The loading of the micellar cores was accomplished by adding varying amounts of a salt precursor, $FeCl_3$ (with molar ratio of functional groups to Fe in the range 4:1–1:2). The salt is preferentially dissolved in the cores of the micelles due to their polar environment. The process takes up to 24 h. After this time, Fe^{3+} cations were reduced by adding a small amount of hydrazine in the presence of air. Thin films of the composite materials were obtained by spin coating the final solution on silicon wafers. A typical thickness of the resulting film is 100 nm. In certain cases, thin films were formed before reduction of the metal.

Chemical changes following 157 nm irradiation of the films were monitored using X-ray photoelectron spectroscopy (XPS) (Physical Electronics Inc. PHI-TFA XPS spectrometer). The diameter of the electron beam was 0.4 mm and analyses were carried out at a depth of 20 nm below the surface. The X-ray source was Al-ka. Elemental composition of the films were analyzed at different depths by XPS depth profiling, involving alternating cycles of sputtering the samples with Ar ions and then acquiring XPS spectra. Ion sputtering was performed with 1 keV Ar ions over an area of 3×3 mm^2. The sputtering velocity was calibrated on a Cr reference sample to be 1 nm/min. After 20 min of sputtering, two high-resolution spectra were acquired at the sample surface in order to follow changes in the binding energies of the XPS peaks due to different chemical species.

VUV surface modification of the non-chemically reduced film was carried out using 157 nm laser light exposure of the films. The use of 157 nm radiation for surface modification of the polymers is justified by the small penetration depth of the 157 nm photons in organic matter ($<$1 nm) [30]. The experimental configuration consists of the laser and the stainless steel 316 chamber with a computer-controlled X–Y–Z–Θ translation stage, where the polymer films were placed. The laser energy falling on the film was controlled with a CaF_2 optical projection system in the Z direction. The sample translator stage had 2 μm translational resolution and repeatability. Different parts of the samples could therefore be exposed under the same conditions. The X–Y–Z–Θ translator was placed and tested inside the stainless steel high vacuum chamber, which was operated over a wide background pressure range ($\sim 10^{-6}$ mbar up to 1 atm). Samples were irradiated at 1 atm background pressure in nitrogen to avoid surface stress from pressure gradients.

The surface morphology of the films was also investigated by a field emission electron microscope (FE-SEM, Supra 35VP) and an atomic force microscope (AFM, Q-Scope250) equipped with a scanner with a maximum scan area of 41×41 μm^2. The cantilever used in the imaging was NSC16 silicon. The microscopes were acoustically and thermally isolated. High-

Please cite this article in press as: E. Sarantopoulou, et al., Self-assembled ferromagnetic and superparamagnetic structures of hybrid Fe block copolymers, Superlattices and Microstructures (2008), doi:10.1016/j.spmi.2007.12.016

resolution images of the film surfaces were obtained on different scanning areas at a maximum scanning rate of 3 Hz with image resolution of 600 × 600 pixels in intermittent contact mode.

Magnetic properties of the samples were investigated using SQUID (MPMS-XL-5, Quantum Design, USA), having high sensitivity (5×10^{-8} emu). The measurements were performed at 5 K and 300 K. Prior to the measurement, samples were magnetized by a field at 6 T. The maximum field applied to the samples was 60 kOe.

3. Results and discussion

The self-assembled structures shaped from reduction, may take the form of lamellas, honeycomb, cubic, or spherical body-centred and a variety of other different structures, depending on parameters such as the type of polymers, the molecular weight, the segment size and the strength of interactions between the blocks. In addition, self-assembled structures appear to be sensitive to the film coating technique and the rate of solvent evaporation [12]. Ordered self-assembly takes place when the conditions for minimum energy and maximum entropy of the system are satisfied. Phase separation can be achieved by ordered self-assembly of macromolecules in the form of micelles, and these provide the conditions for nano-scale patterning.

Self-assembled processes can be further catalyzed by the presence of metallic functional groups, which under specific conditions and chemical reactions allow formation of metallic micro or nanostructures [28].

This has been explained by the fact that the dimensions of the self-assembled metallic nanoparticles are smaller than the dimensions of magnetic domains (from the exchange and magnetic interactions between atoms). Therefore, no interaction occurs between spins from different atoms in the total magnetism of the nano-domains (i.e. ferromagnetism is not present). The magnetic nanoparticles are free to be aligned with respect to an external magnetic field above the critical temperature (blocking temperature), while below this temperature, the magnetization behavior shifts from superparamagnetic to ferromagnetic. This shift is caused by the thermal energy overcoming the magnetic anisotropy energy barrier of single-domain particles. Since the magnetic properties (coercivity, remnant magnetization, and blocking temperature) strongly depend on the exchange and magnetic dipole atomic interactions, the material behaves as a homogeneous thin film with ferromagnetic response for strong interactions. The correlation and distinction between the ferromagnetic and superparamagnetic responses of metallic nanoparticles in polymeric matrices are not fully understood. The response appears to depend on many parameters, such as size and type of metal-nanoparticles, morphological surface and volume configurations and self-assembled structuring.

3.1. Chemical reduction

SEM images of surface morphology of chemically reduced S2VP films (loaded with $FeCl_3$ precursor) on Si/Ta substrates are shown in Fig. 1. Micelle-like nanoparticle islands rich in iron [11] were formed with average dimensions of ∼30 nm, (average value of distribution of diameters of 90% of nanoparticles).

Further aggregation is expected to be limited because the S2VP polymer forms a micelle-like nano-cage around the iron nanoparticles by physical adsorption and chemical bonding [12]. More specifically, the repulsive electrostatic forces between the micelles prevent further agglomeration of the iron islands, despite the fact that larger micelle-like structures of ∼100 nm average size

Please cite this article in press as: E. Sarantopoulou, et al., Self-assembled ferromagnetic and superparamagnetic structures of hybrid Fe block copolymers, Superlattices and Microstructures (2008), doi:10.1016/j.spmi.2007.12.016

Q1

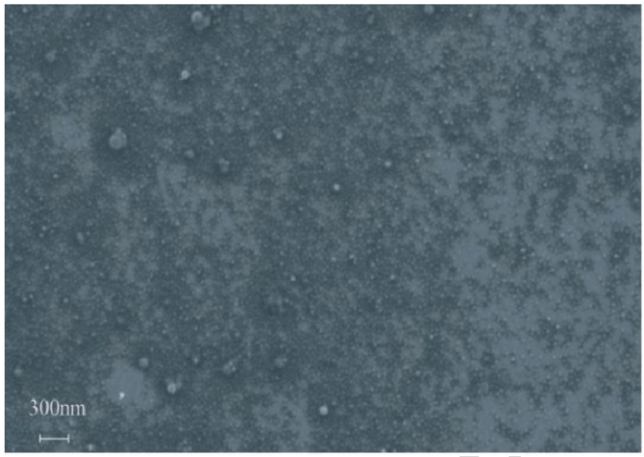

Q2 Fig. 1. SEM image of micelle-like structures in PS–P2VP/$FeCl_3$ hybrid film following chemical reduction. The average dimension of the nanoparticles is ∼30 nm, (average value of distribution of diameters of 90% of nanoparticles).

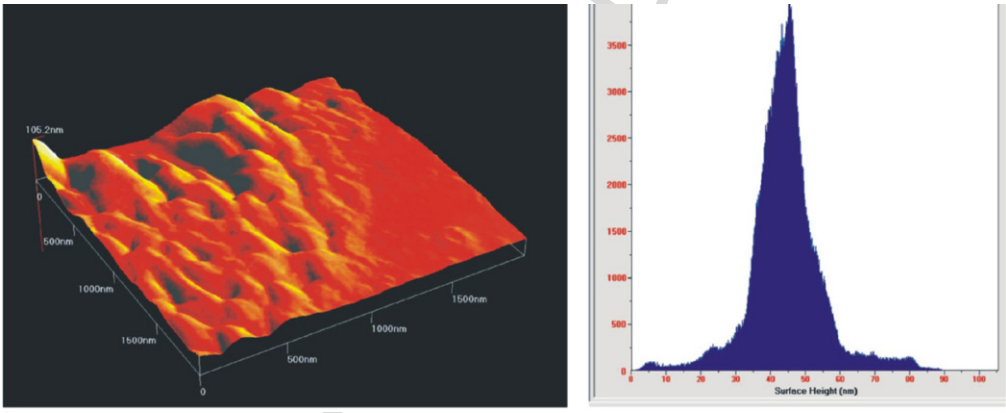

Fig. 2. AFM image of the PS–S2VP/$FeCl_3$ hybrid film. The typical surface roughness is ∼45 nm for the scanned area of 1.7 μm × 1.7 μm (average value of distribution of diameters of 90% of nanoparticles).

were sometimes formed. In certain cases these larger micelles spontaneously aggregate to form structures larger than 100 nm. From the AFM image of Fig. 2 (1.7 μm × 1.7 μm, AFM scanned area), the particles have nearly spherical morphology and the typical surface roughness is about −45 nm, (average value of distribution of diameters of 90% of nanoparticles), in agreement with the SEM image of Fig. 1. An AFM image of the SVP copolymer in toluene solvent coated on a Si/Ta substrate, before the loading of the micellar cores, is shown in Fig. 3. The surface morphology is of this sample is different and the roughness is 5–10 nm (1.2 μm × 1.2 μm, AFM scanned area). From these images it is clear that adding $FeCl_3$ catalyzes the formation of metallic nanostructures.

XPS was used to study the chemical composition of the nanostructures formed on the polymer matrix. Analysis of the Fe 2p peak was carried out on the samples produced by chemical reduction; the spectrum obtained after 20 min of sputtering is shown in Fig. 4. The binding energy of Fe $2p^{3/2}$ at the surface was 711 eV and after sputtering was shifted to 708 eV. We therefore

Please cite this article in press as: E. Sarantopoulou, et al., Self-assembled ferromagnetic and superparamagnetic structures of hybrid Fe block copolymers, Superlattices and Microstructures (2008), doi:10.1016/j.spmi.2007.12.016

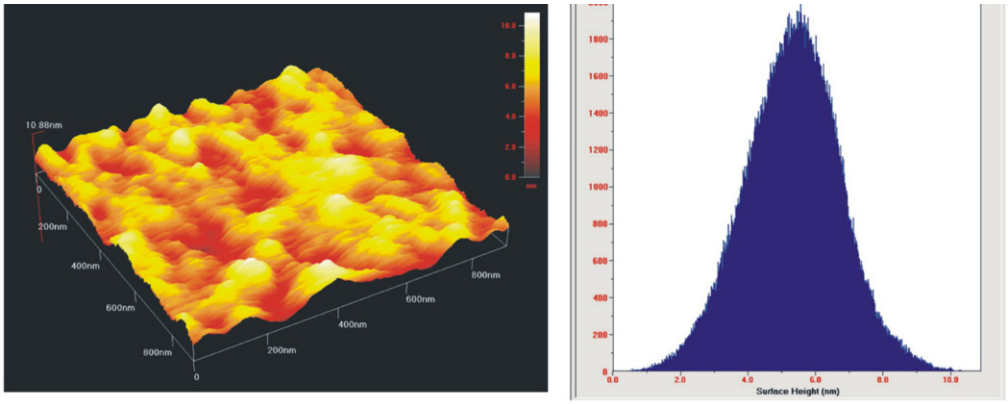

Fig. 3. AFM image of the PS–S2VP copolymer in toluene solvent spin-coated on a Si/Ta substrate, before the loading of the micellar cores. (AFM scanned area 1.2 μm × 1.2 μm). The surface roughness is 5 nm, (average value of distribution of diameters of 90% of nanoparticles).

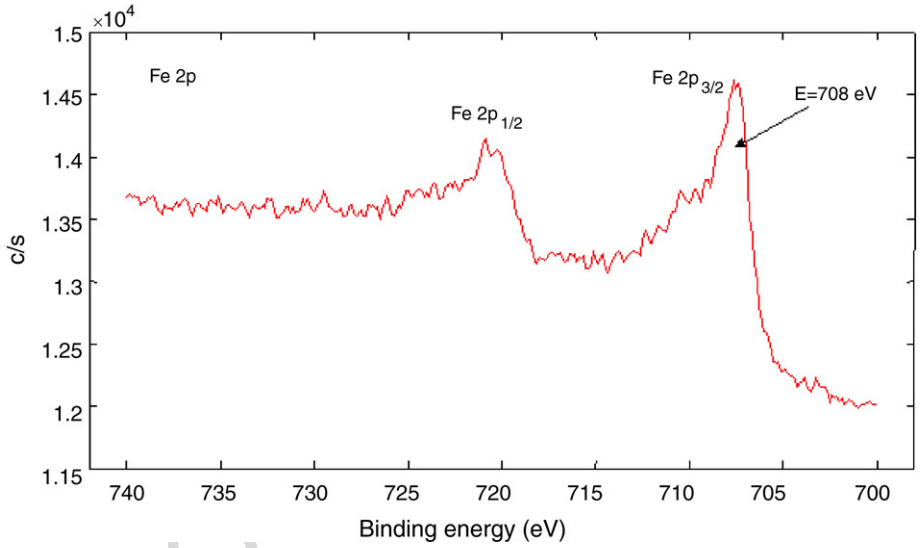

Fig. 4. XPS spectra of the Fe 2p peak in the samples produced by chemical reduction after 20 min of sputtering.

conclude that the Fe atoms on the surface are bonded as iron oxide, while the bulk contains Fe atoms with metallic bonding character. The presence of surface oxide is reasonable since the entire process was conducted in air. The obtained XPS spectrum is in agreement with the results of Chen et al. [10], who concluded that after the reducing step, Fe^{3+} has been reduced to metallic Fe(0) and Fe(II), perhaps due to incomplete reduction, with some products also coordinated with nitrogen.

XPS spectra taken after 20 min of sputtering, showing the N 1s peak in samples produced by chemical reduction, are shown in Fig. 5. At the surface, this peak has a binding energy of 401 eV, assigned to oxidized or adsorbed N-based species. After sputtering, the binding energy beneath the surface is 399 eV, suggesting that nitrides such as Fe–N were formed. Depth profile XPS

Please cite this article in press as: E. Sarantopoulou, et al., Self-assembled ferromagnetic and superparamagnetic structures of hybrid Fe block copolymers, Superlattices and Microstructures (2008), doi:10.1016/j.spmi.2007.12.016

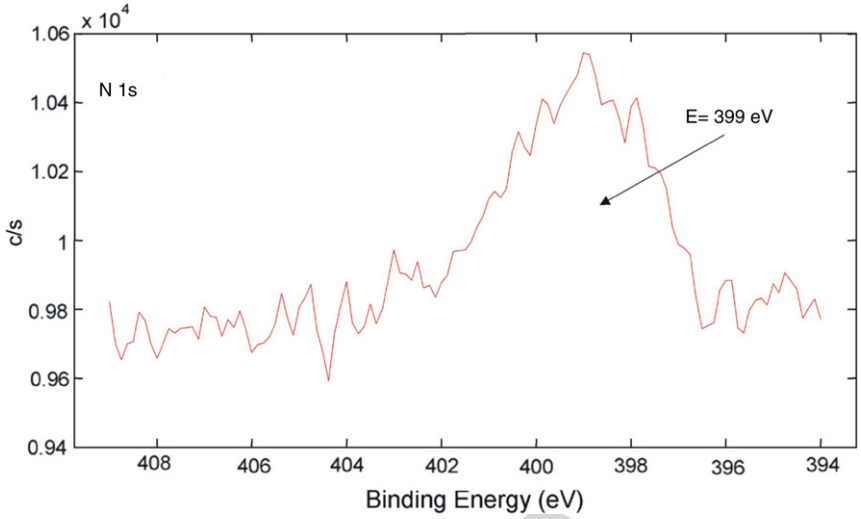

Fig. 5. XPS spectra of the N 1s peak in the samples produced by chemical reduction after 20 min of sputtering.

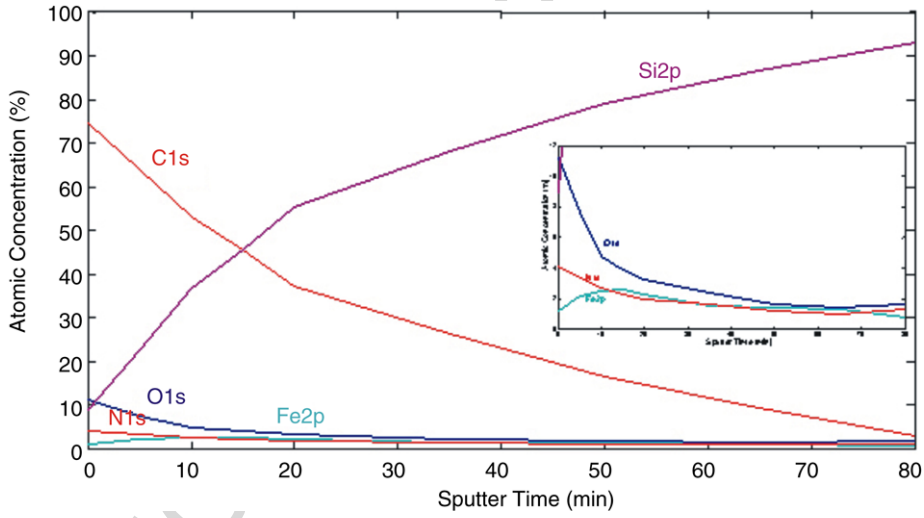

Fig. 6. XPS depth profile of the S2VP film after chemical reduction. In the inset, the depth profile is shown with a magnification of the *y*-axis. C, O, Fe and N were found in the film surface. Beneath the film, the Si peak from the Si substrate is visible.

spectra reveal the presence of nitride (based on the N 1s peak position), Fe(0) and Fe(II). In the bulk film, the iron metallic state was predominant, while the surface contained mainly Fe(II).

The XPS depth profile of the S2VP sample is shown in Fig. 6. The C, O, Fe and N elements have higher concentration at the film surface. The C concentration sharply decreases up to 80 nm depth. The O concentration decreases up to 10 nm and then remains constant, perhaps due to the surface oxidization when the film was removed from the nitrogen chamber. The VUV light chemically modifies the surface, within a penetration depth of few tens of nanometers. The degree of chemical modification, and thus oxidization, is inversely proportional to the

Please cite this article in press as: E. Sarantopoulou, et al., Self-assembled ferromagnetic and superparamagnetic structures of hybrid Fe block copolymers, Superlattices and Microstructures (2008), doi:10.1016/j.spmi.2007.12.016

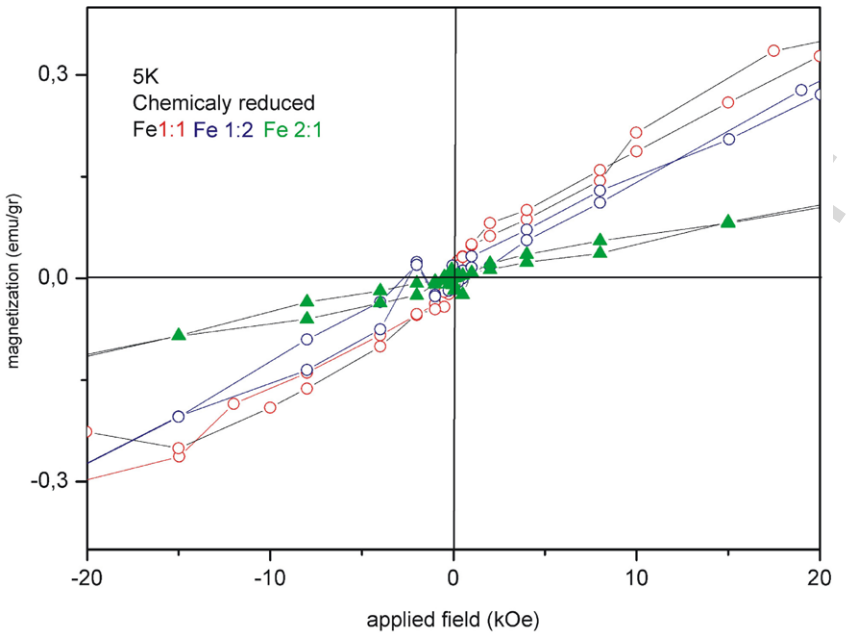

Fig. 7. Superparamagnetic response of the chemically reduced films at 300 K. The applied magnetic field is in the plane of the samples.

penetration depth. The Fe concentration increases up to 10 nm depth and then remains constant. The iron concentration is increased for the same depth to compensate the changes of the chemical potentials.

Finally, the magnetic response of chemically reduced films at 5 K is shown in Fig. 7. A superparamagnetic response is observed with nearly zero coercivity and remanence for all Fe concentrations. The coercivities are 26, 15 and 8 Oe for Fe ratios of 2:1, 1:1 and 1:2 respectively. Small magnetic particles below a critical size are known to be single-domain particles due to the interaction between the magnetic dipole fields and wall domains [31]. Iron nanoparticles formed by chemical reduction consist of single magnetic domains, so the origin of the small magnetic hysteresis must be due only to exchange interactions. In addition, single-domain particles exhibit superparamagnetic properties at higher temperatures because the thermal energy exceeds the magnetic anisotropy energy of the magnetic domains [25]. The critical size of single-domain Fe spherical particles has been estimated to be 14 nm, and for the iron oxides 128 and 166 nm [25].

3.2. 157 nm laser reduction

In the case of reduction with laser radiation, the formation of iron oxide is not expected since this process was conducted in nitrogen [11]. EDXS microanalyses of the exposed areas at 157 nm revealed the presence of iron, and the concentration of iron was enhanced in the irradiated areas, which showed an aggregation-like morphology [11].

For the films reduced by 157 nm irradiation, the magnetic responses at 5 K and 300 K are shown in Fig. 8. An external magnetic field was applied along the plane of the films. At 300 K, the magnetization of the film increases at higher external magnetic field without saturation. Clearly, this is due to a superparamagnetic response because the thermal energy exceeds the magnetic

Please cite this article in press as: E. Sarantopoulou, et al., Self-assembled ferromagnetic and superparamagnetic structures of hybrid Fe block copolymers, Superlattices and Microstructures (2008), doi:10.1016/j.spmi.2007.12.016

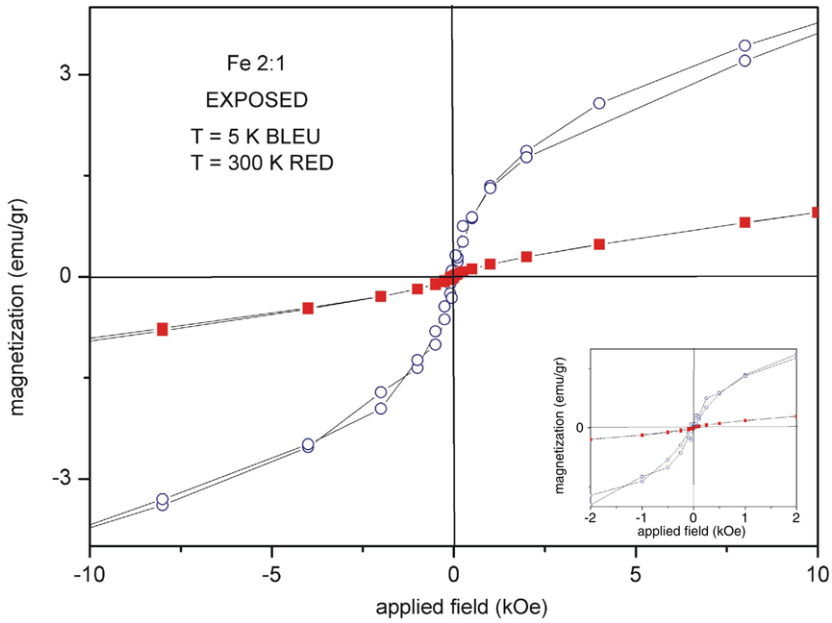

Fig. 8. The magnetization curve versus applied field for the VUV reduced films at 5 K and 300 K. The applied magnetic field is in the plane of the samples.

anisotropy energy at room temperature. In this case, the hysteresis indicates small remanence (M_r) and a coercivity of $H_c \sim 50$ Oe. This response indicates the absence of long-range magnetic dipole interactions among the assemblies of the iron nanoparticles. At 5 K, the magnetization of the films increases and exhibits a symmetric and enlarged hysteresis loop, suggesting a transition from the superparamagnetic to ferromagnetic state. At 5 K, the coercivity increases to ~100 Oe.

Anisotropic particles can be single-domain particles at larger dimensions than their spherical counterparts [25]. One source of anisotropy is external stress during annealing in an external magnetic field, ion beam or laser irradiation. As reported previously, laser irradiation can be used to control the fabrication of ferromagnetic dots with an average size of 10 nm based on the melting of the film over a short period of time [32]. The films in that case are superparamagnetic at room temperature and ferromagnetic at 10 K. This result is consistent with the present work, in which irradiation at 157 nm locally changes the morphology and the stoichiometry of the films [12]. The induced strain increases the single-domain critical dimensions, allowing for a ferromagnetic response at 5 K for nanoparticles of average size 5–10 nm that are formed during laser irradiation of the film surface. Examples of these films are shown in the AFM images of Fig. 9.

The magnetic response at 5 K of the irradiated films with different iron concentrations is given in Fig. 10 for fields up to 10 kOe. The coercivities up to 1.2 kOe are 99, 74 and 60 Oe for iron ratios of Fe 2:1, 1:1 and 1:2, respectively. A similar response is expected at longer VUV wavelengths and for different polymers [33–36].

4. Conclusion

Self-assembled structures on thin films of block copolymer/Fe hybrid materials were fabricated on Si/Ta substrates, either by wet chemistry or laser vacuum ultraviolet light

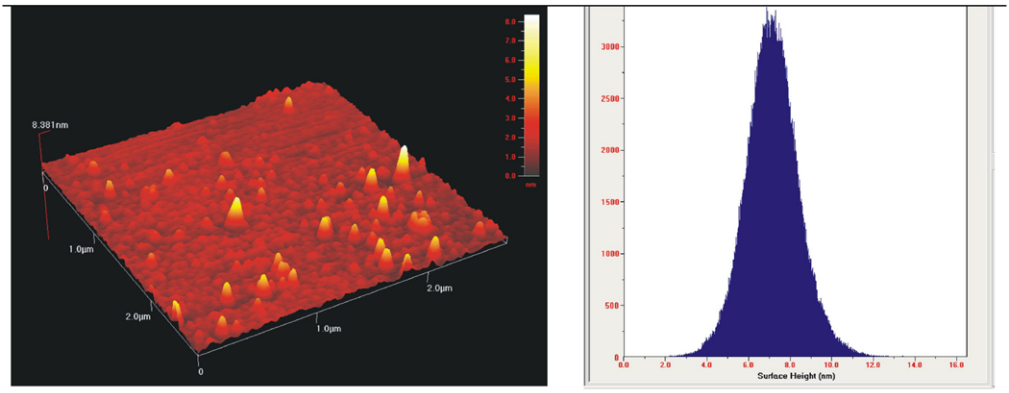

Fig. 9. AFM image of the VUV light reduced films. The edge between light exposed and non-exposed areas is indicated. The exposed surface has higher microscale roughness than the non-exposed surface. However, molecular photodissociation and rearrangement on the processed areas limits the size of the iron nanostructures to 7 nm, (average value of distribution of diameters of 90% of nanoparticles).

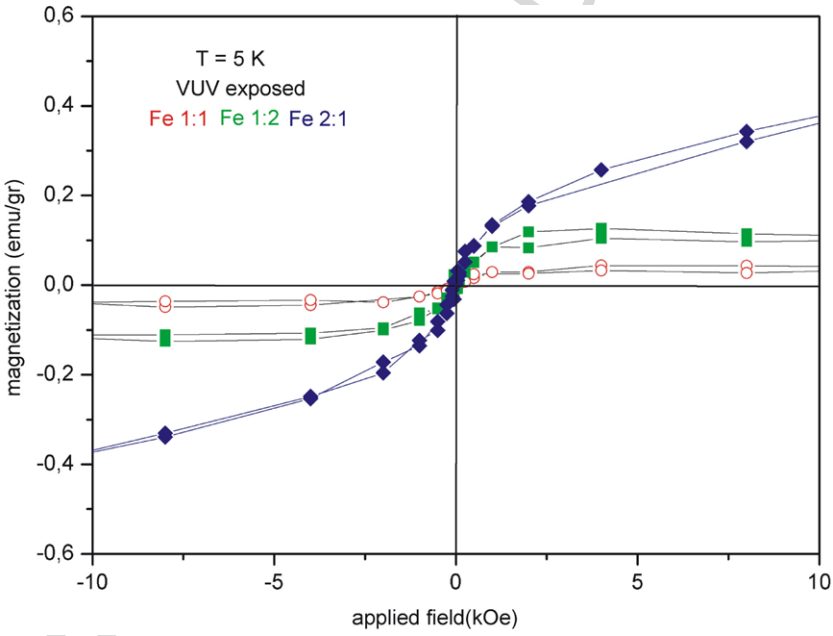

Fig. 10. Ferromagnetic responses at 5 K of the irradiated films with different iron concentrations for fields up to 10 kOe. The coercivities up to 1.2 kOe are 99, 74 and 60 Oe for iron ratios of 2:1, 1:1 and 1:2 respectively.

processing at 157 nm. In both cases, XPS analysis reveals the presence of metallic-like iron in the 2p state. In addition, XPS depth profiles reveal metallic iron and Fe(II) bonding. The films reduced by 157 nm show a ferromagnetic response at 5 K and a superparamagnetic response at room temperature, while the chemically reduced films are superparamagnetic for both temperatures. The ferromagnetic response of the VUV light reduced films is attributed to the formation of 5–10 nm metallic iron nanostructures.

Please cite this article in press as: E. Sarantopoulou, et al., Self-assembled ferromagnetic and superparamagnetic structures of hybrid Fe block copolymers, Superlattices and Microstructures (2008), doi:10.1016/j.spmi.2007.12.016

References

[1] M.A. El-Sayed, Acc. Chem. Res. 34 (2001) 257.
[2] S. Sun, S. Anders, T. Thomson, J.E.E. Baglin, M.F. Toney, H.F. Hammann, C.B. Murray, B.D. Tertis, J. Phys. Chem. B 107 (2003) 5419.
[3] T. Trindade, P. O'Brien, N.L. Picket, Chem. Mater. 13 (2001) 3843.
[4] M.C. Daniel, D. Astruc, Chem. Rev. 104 (2003) 293.
[5] S. Sun, C.B. Murray, D. Weller, L. Folks, A. Moser, Science 287 (2000) 1989.
[6] (a) J.I. Abes, R.E. Cohen, C.A. Ross, Mater. Sci. Eng. C 23 (2003) 641;
(b) Y.S. Kang, S. Risbud, J.F. Rabolt, P. Stroeve, Chem. Mater. 8 (1996) 2209.
[7] M. Chen, S. Yamamuro, D. Farrell, S.A. Majetich, J. Appl. Phys. 93 (2003) 7551.
[8] (a) C.C. Berry, A.C.G Curtis, J. Phys. D: Appl. Phys. 36 (2003) R198;
(b) C.C. Berry, J. Mater. Chem. 15 (2005) 543.
[9] P. Tartaj, M. del Puerto Morales, S. Veintemillas-Verdaguer, T. Gonzalez-Carreno, C.J. Serna, J. Phys. D: Appl. Phys. 36 (2003) R182.
[10] (a) L. Chen, W.J. Yang, C.Z. Yang, J. Mater. Sci. 32 (1997) 3571;
(b) L. Chein, K. Liu, C.Z. Yang, Polym. Bull. 37 (1996) 377.
[11] Z. Guo, L.L. Henry, V. Palshin, E.J. Podlha, J. Mater. Chem. 16 (2006) 1772.
[12] E. Sarantopoulou, K. Gatsouri, Z. Kollia, S. Pispas, S. Kobe, J. Kovač, Phys. Status Solidi (2007) (in press).
[13] M. Rutnakornituk, M.S. Thompson, L.A. Harris, K.E. Farmer, A.R. Esker, J.S. Riffle, J. Connally, T.G. St Pierre, Polymer 43 (2002) 2337.
[14] K. Kurihara, J. Kizlig, P. Stenius, J.H. Fendler, J. Am. Chem. Soc. 105 (1983) 2574.
[15] M. Harada, H. Einaga, Langmuir 22 (2006) 2371.
[16] R.G. Song, M. Yamaguchi, O. Nishimura, M. Suzuki, Appl. Surf. Sci. 253 (2007) 3093.
[17] (a) M. Yoon, Y.M. Kim, Y. Kim, V. Volkov, H.J. Song, Y.J. Park, S.L. Vasilyak, I.-W. Park, J. Magn. Magn. Mater. 265 (2003) 357;
(b) M. Yoon, Y. Kim, Y.M. Kim, H. Yoon, V. Volkov, A. Avilov, Y.J. Park, I.W. Park, J. Magn. Magn. Mater. 272–276 (2004) e1259.
[18] I. Narita, T. Oku, H. Tokoro, K. Suganuma, J. Electron. Microsc. 55 (2006) 123.
[19] B.H. Sohn, R.E. Cohen, G.C. Papaefthymiou, J. Magn. Magn. Mater. 182 (1998) 216.
[20] J.M. Petroski, Z.L. Wang, T.C. Green, M.A. El Sayed, J. Phys. Chem. B 102 (1998) 3316.
[21] H. Shao, H. Lee, Y. Huang, I. Ko, C. Kim, IEEE Trans. Magn. 41 (2005) 3388.
[22] S.I. Hirano, T. Yogo, W. Sakamoto, S. Yamada, T. Nakamura, T. Yamammto, H. Ukai, K. Banno, T. Nakafuku, Y. Ando, J. Sol–Gel Sci. Technol. 26 (2003) 35.
[23] T. Sato, H. Haneda, M. Seki, T. Iijima, Appl. Phys. A 50 (1990) 13.
[24] L. Motte, F. Billoudet, E. Lacaze, J. Douin, M.P. Pelini, J. Phys. Chem. B 101 (1997) 138.
[25] D.L. Leslie Pelecky, R.D. Dieke, Chem. Mater. 8 1996 (1770).
[26] J. Knipping, H. Wiggers, B.F. Kock, T. Hulser, B. Rellinghaus, P. Roth, Nanotechnology 15 (2004) 1665.
[27] (a) J.P. Spatz, S. Sheiko, M. Möller, Macromolecules 29 (1996) 3220;
(b) J.P. Spatz, A. Roescher, M. Möller, Adv. Mater. 8 (1996) 337.
[28] K.E. Gonsalves, G. Carlson, M. Benaissa, M. Jose-Yacaman, D.Y. Kim, J. Kumar, J. Mater. Chem. 7 (1997) 703.
[29] (a) N. Hadjichrisitidis, H. Iatrou, S. Pispas, M. Pitsikalis, J. Polym. Sci: Part A: Polym. Chem. 38 (2000) 3211;
(b) S. Pispas, J. Phys. Chem. B 110 (2006) 2649;
(c) D. Topouza, K. Orfanou, S. Pispas, J. Polym. Sci. Part A: Polym. Chem. 42 (2004) 6230.
[30] Z. Kollia, E. Sarantopoulou, A.C. Cefalas, S. Kobe, Appl. Surf. Sci. 248 (2005) 248.
[31] S. Morup, Europhys. Lett. 28 (1994) 671.
[32] J.Y. Yang, K.S. Yoon, Y.H. Do, J.H. Kim, J.H. Lee, C.O. Kim, J.P. Hong, E.K. Kim, IEEE Trans. Magn. 41 (2005) 3313.
[33] V. Bellas, E. Tegou, I. Raptis, E. Gogolides, P. Argitis, H. Iatrou, N. Hadjichristidis, E. Sarantopoulou, A.C. Cefalas, J. Vac. Sci. Technol. B 20 (2002) 2902.
[34] A.C. Cefalas, M.A. Dubinskii, E. Sarantopoulou, R.Yu. Abdulsabirov, S.L. Korableva, A.K. Naumov, V.V. Semashko, C.A. Nicolaides, Laser Chem. 13 (1993) 143.
[35] E. Sarantopoulou, Z. Kollia, A.C. Cefalas, Microelectron. Eng. 53 (2000) 105.
[36] E. Sarantopoulou, Z. Kollia, A.C. Cefalas, M.A. Dubinskii, C.A. Nicolaides, R.Yu. Abdulsabirov, S.L. Korableva, A.K. Naumov, V.V. Semashko, Appl. Phys. Lett. 65 (1994) 813.

Q3

Please cite this article in press as: E. Sarantopoulou, et al., Self-assembled ferromagnetic and superparamagnetic structures of hybrid Fe block copolymers, Superlattices and Microstructures (2008), doi:10.1016/j.spmi.2007.12.016